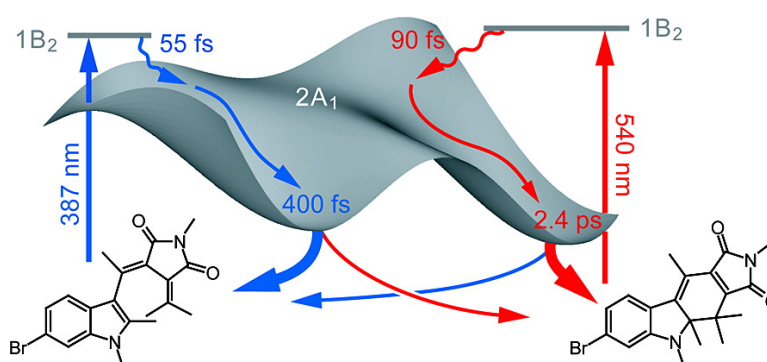


Comparing a Photoinduced Pericyclic Ring Opening and Closure: Differences in the Excited State Pathways

Björn Heinz, Stephan Malkmus, Stefan Laimgruber, Steffen Dietrich, Christine Schulz, Karola Rck-Braun, Markus Braun, Wolfgang Zinth, and Peter Gilch

J. Am. Chem. Soc., **2007**, 129 (27), 8577-8584 • DOI: 10.1021/ja071396i • Publication Date (Web): 14 June 2007

Downloaded from <http://pubs.acs.org> on February 16, 2009



More About This Article

Additional resources and features associated with this article are available within the HTML version:

- Supporting Information
- Links to the 5 articles that cite this article, as of the time of this article download
- Access to high resolution figures
- Links to articles and content related to this article
- Copyright permission to reproduce figures and/or text from this article

[View the Full Text HTML](#)

Comparing a Photoinduced Pericyclic Ring Opening and Closure: Differences in the Excited State Pathways

Björn Heinz,[†] Stephan Malkmus,[†] Stefan Laimgruber,[†] Steffen Dietrich,[‡] Christine Schulz,[‡] Karola Rück-Braun,[‡] Markus Braun,[†] Wolfgang Zinth,[†] and Peter Gilch^{*†}

Contribution from the Department für Physik — Munich Center for Integrated Protein Science, Ludwig-Maximilians-Universität, Oettingenstrasse 67, D-80538 München, Germany, and Institut für Chemie, Technische Universität Berlin, Strasse des 17. Juni 135, D-10623 Berlin, Germany

Received February 27, 2007; E-mail: peter.gilch@physik.uni-muenchen.de.

Abstract: The photochromicity of fulgimides rests on the existence of open (E) and closed ring (C) isomers. As predicted by the Woodward–Hoffmann rules both isomers can photochemically be interconverted. This interconversion has been studied by femtosecond fluorescence and transient absorption spectroscopy. For either direction (E → C cyclization and C → E cycloreversion) a biphasic fluorescence decay on the 0.1–1 ps time scale is observed. The longer time constants of the decays equal the formation times of the photoproducts. The time constants retrieved (0.06 and 0.4 ps for E → C, 0.09 and 2.4 ps for C → E) and the associated spectral signatures differ substantially. This indicates that no common excited-state pathway for the two directions exists, as one would infer from a simple Woodward–Hoffmann consideration. These findings support recent quantum dynamic calculations on the excited-state topology of fulgimides.

1. Introduction

About 40 years ago R. B. Woodward and R. Hoffmann formulated their rules on the conservation of orbital symmetry during pericyclic chemical reactions.¹ Their stereochemical predictions of the outcome of a pericyclic reaction had and still have a huge impact on the preparative organic chemistry. Here, among the most famous examples are probably the total synthesis of vitamin B₁₂ and the industrial as well as the epidermal synthesis of vitamin D where the key steps are photoinduced pericyclic reactions.^{2,3} In the latter case a cyclohexadiene (CHD) moiety in a sterine is converted into a hexatriene (HT) motive by a ring-opening reaction. The ring-opening and -closure reactions of the bare CHD/HT system often serve as textbook examples for the validity of the Woodward–Hoffmann rules and have thus been studied intensively.^{4–8}

Within the framework of these rules the transformation of electronic states along a reactive coordinate is considered (see Figure 1(a)). This reactive coordinate connects the reactant with

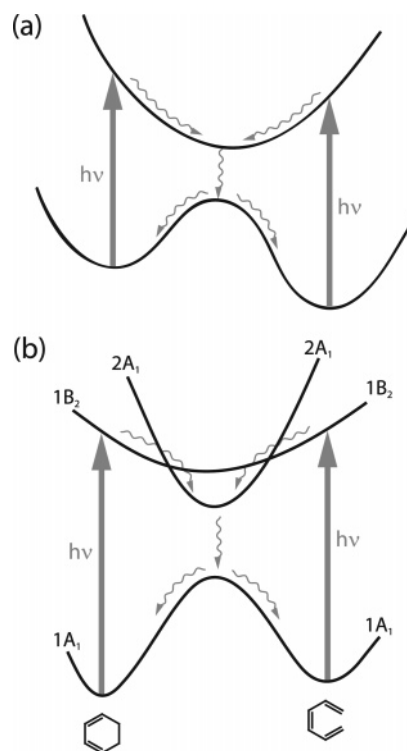


Figure 1. (a) Schematic for a one-dimensional photochemical reaction pathway where both isomers utilize a common excited-state potential-energy surface. (b) Reaction model for the CHD/HT system as proposed in the literature^{4,6} involving two excited states.

the product and conserves a symmetry element like a C₂ axis or a mirror plane.¹ Nevertheless, the product stereochemistry is often reliably predicted even for systems lacking such

[†] Ludwig-Maximilians-Universität.

[‡] Technische Universität Berlin.

- (1) Woodward, R. B.; Hoffmann, R. *Angew. Chem., Int. Ed. Engl.* **1969**, *8*, 781–853.
- (2) Yamada, Y.; Miljkovič, W.; Wehrli, P.; Golding, B.; Loliger, P.; Keese, R.; Müller, K.; Eschenmoser, W. *Angew. Chem., Int. Ed. Engl.* **1969**, *8*, 343–348.
- (3) Butenandt, A. *Angew. Chem., Int. Ed. Engl.* **1960**, *72*, 644–650.
- (4) Fuss, W.; Schmid, W. E.; Trushin, S. A. *J. Chem. Phys.* **2000**, *112*, 8347–8362.
- (5) Pullen, S. H.; Anderson, N. A.; Walker, L. A.; Sension, R. J. *J. Chem. Phys.* **1998**, *108*, 556–563.
- (6) Hofmann, A.; de Vivie-Riedle, R. *J. Chem. Phys.* **2000**, *112*, 5054–5059 and references therein.
- (7) Geppert, D.; Seyfarth, L.; de Vivie-Riedle, R. *Appl. Phys. B* **2004**, *79*, 987–992.
- (8) Tamura, H.; Nanbu, S.; Ishida, T.; Nakamura, H. *J. Chem. Phys.* **2006**, *125*, 034307 and references therein.

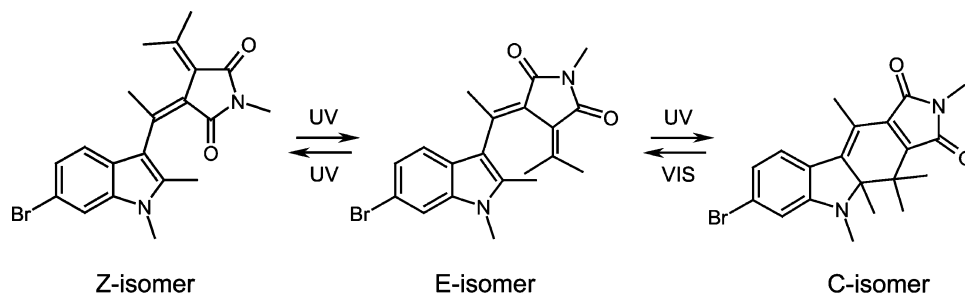


Figure 2. Structures of the photoisomers of the investigated *N*-methyl-indolyl-fulgimide.

symmetry elements. A photochemically allowed pericyclic reaction pathway is forbidden in the ground state because of a prohibitively large barrier resulting from an avoided crossing of electronic states of equal symmetry. For a photoreversible reaction this implies a scheme like the one shown in Figure 1a which is often used to describe photochemical reactions.⁹ On the basis of semiempirical calculations van der Lugt and Oosterhoff proposed an extension of this simple model for pericyclic reactions in 1969¹⁰ that was later adapted to describe the photophysics of the CHD/HT system (Figure 1b). In addition to the ground state ($1A_1$) it involves two electronically excited states: One is optically bright ($1B_2$) and the other one is a dark state ($2A_1$), which twice crosses the $1B_2$ surface. The $2A_1$ state is the one which in the Woodward–Hoffmann sense correlates with the ground state. It has to be stressed that in both models the branching point of the respective photoreactions is the minimum of the lowest excited state. This bears the consequence that the forward and the backward reaction pathways both pass through the same region of this very potential energy surface. Over the last decades growing computational power made it possible to calculate excited-state reaction pathways which led to a further refinement of these models. These studies stress the importance of multidimensional reactive spaces and of conical intersections mediating the transitions between electronic states.¹¹ Conical intersections have been located by means of ab initio calculations in many systems undergoing pericyclic photoreactions and are believed to be responsible for the ultrafast nature of many of these reactions.^{12,13}

Experimental^{4,5} and theoretical studies^{6,8} on the prototypical CHD \rightarrow HT ring-opening reaction afforded a reaction scheme like the one shown in Figure 1b. Here, excitation of the CHD $1A_1$ ground state to the optically bright $1B_2$ state is followed by rapid internal conversion via a conical intersection to the dark $2A_1$ state.⁶ This $2A_1$ state is of doubly excited nature and encounters another conical intersection with the $1A_1$ ground state which, as mentioned above, is the branching point between product (HT) formation and back reaction yielding the starting material. This proposed model has received experimental support by means of femtosecond spectroscopy. Here, characteristic times of 50 fs and \sim 250 fs have been observed and assigned to

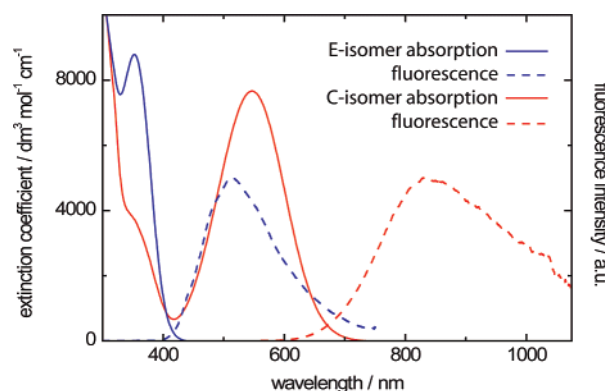


Figure 3. Steady-state UV–vis absorption (solid lines) and fluorescence spectra (dashed lines) of the E-isomer (blue) and the C-isomer (red).

the $1B_2 \rightarrow 2A_1$ internal conversion and HT product formation, respectively.^{4,5} In consistency with these results very similar time constants for both processes were found for the HT \rightarrow CHD backward reaction taking place after excitation of HT as shown by another experimental study.¹⁴ An elaborate theoretical approach for the CHD/HT system has been made by de Vivie-Riedle and co-workers introducing two reactive coordinates.⁶ The potential energy surface used in that model features two conical intersections connecting the lowest excited and the ground state.

With the present study we want to contribute to the question if the CHD/HT system can serve as a model for a technologically relevant photoreactive molecule containing this moiety as the reactive center. For this purpose we have investigated an indolyl-substituted fulgimide (structure depicted in Figure 2). Similar to the chemically related diarylethenes,¹⁵ fulgimides and fulgides^{16–18} have recently received attention as molecular switches, especially as promising candidates for fast optical data storage with nondestructive readout. Fulgimides are photochromic compounds with thermally stable isomers featuring well separated absorption bands for the open (E) and closed (C) ring isomers thanks to suitable chemical modification (see Figure 3).^{16,19,20} Only the C-isomer features an absorption band in the visible peaking around 550 nm. Irradiation of the C-isomer in this spectral range yields the E-isomer. In the course of this C

(9) Turro, N. J., Ed. *Modern Molecular Photochemistry*; The Benjamin/Cummings Publishing Co., Inc.: Menlo Park, CA, 1978.
 (10) van der Lugt, W. T. A. M.; Oosterhoff, W. *J. Am. Chem. Soc.* **1969**, *91*, 6042–6049.
 (11) Klessinger, M.; Michl, J., Eds. *Excited states and photochemistry of organic molecules*; VCH Publishers: Basel, Cambridge, New York, Weinheim, Germany, 1995 and references therein.
 (12) Bernardi, F.; De, S.; Olivucci, M.; Robb, M. A. *J. Am. Chem. Soc.* **1990**, *112*, 1737–1744.
 (13) Bernardi, F.; Olivucci, M.; Robb, M. A. *Chem. Soc. Rev.* **1996**, *25*, 321–328.

(14) Anderson, N. A.; Durfee, C. G.; Murnane, M. M.; Kapteyn, H. C.; Sension, R. *J. Chem. Phys. Lett.* **2000**, *323*, 365–371.
 (15) Irie, M. *Chem. Rev.* **2000**, *100*, 1685–1716.
 (16) Yokoyama, Y. *Chem. Rev.* **2000**, *100*, 1717–1739.
 (17) Seibold, M.; Port, H. *Chem. Phys. Lett.* **1996**, *252*, 135–140.
 (18) Liang, Y. C.; Dvornikov, A. S.; Rentzepis, P. M. *Proc. Natl. Acad. Sci. U.S.A.* **2003**, *100*, 8109–8112.
 (19) Wolak, M. A.; Thomas, C. J.; Gillespie, N. B.; Birge, R. R.; Lees, W. J. *J. Org. Chem.* **2003**, *68*, 319–326.
 (20) Otto, B.; Rück-Braun, K. *Eur. J. Org. Chem.* **2003**, *13*, 2409–2417.

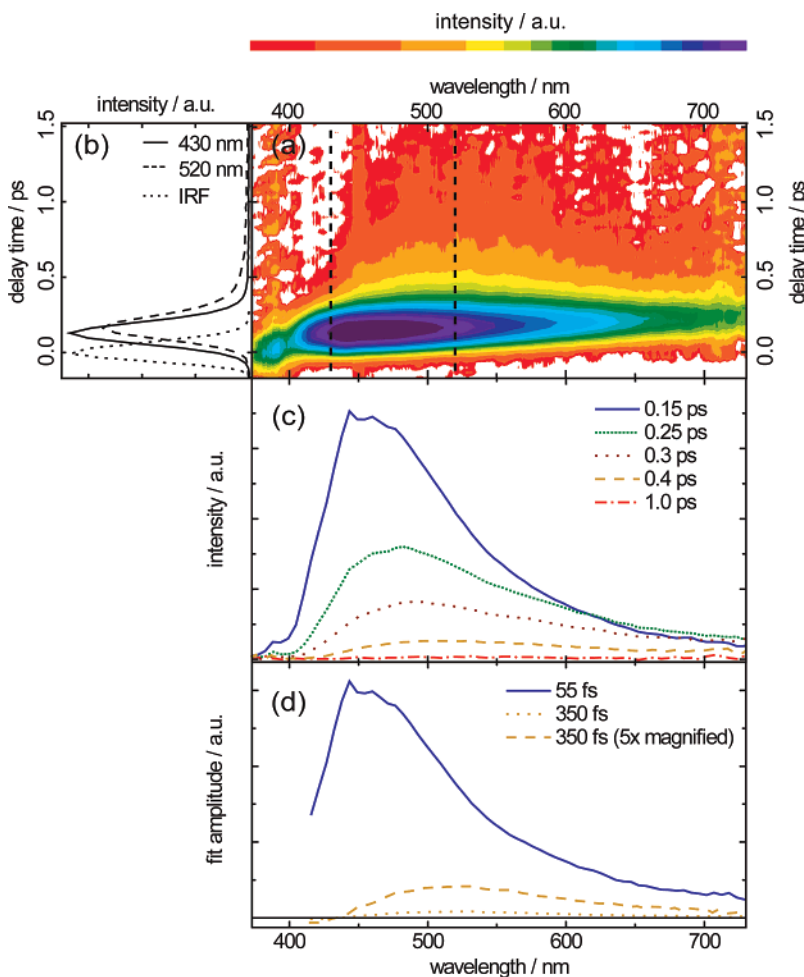


Figure 4. Femtosecond fluorescence experiment on the E-isomer after excitation at 387 nm. (a) Contour plot of the transient fluorescence. The dashed lines indicate the wavelengths which are plotted in panel b. (b) Decay of the signal at 430 nm (solid line) and 520 nm (dashed line). The instrumental response function (IRF) is shown as a dotted line. (c) Transient fluorescence spectra at delay times as indicated. The spectral signatures at 387 and 438 nm at early delay times are due to excitation light and Raman scattering of the solvent, respectively. (d) Decay-associated spectra of the time constants retrieved from a global analysis. For better perception an enlarged spectrum of the 350 fs time constant is also plotted (dashed yellow line).

→ E ring-opening reaction the visible band is completely bleached. The E-isomer undergoes light induced cyclization reverting to the C-form and E-Z isomerization around the C=C bond connecting both rings (Figure 2). The quantum yield of the latter reaction η_Z has been determined in chemically very similar indolyl-fulgimides and was found to be much smaller than the quantum yield for the cyclization η_C with a ratio of η_C/η_Z ranging from 14 to 50.¹⁹ (Please note that the ring closure of the molecules investigated in that reference formally is the Z → C reaction.) These results give a strong indication that the E-Z isomerization plays only a minor role for the photochemistry of the E-isomer and we thus assume that this reaction can be neglected in the discussion of our results. A previous time-resolved study on the E → C ring closure of a fulgimide reports on picosecond dynamics and discusses the possible involvement of an intermediate state which has not been further characterized.¹⁸ The ring closure of a fulgide has been studied in solution²¹ and in a polymer matrix.²² In solution a branched reaction scheme has been proposed involving a direct reaction pathway and one via an intermediate state with a lifetime greater

than or equal to 10 ps.²¹ However, no evidence for the existence of an intermediate could be found in the polymer matrix,²² and the involvement of such a state remains unclear. The ring-opening reaction of the fulgimide shown in Figure 2 has recently been investigated by our group with ultrafast transient absorption and IR spectroscopy.^{23,24} Here, evidence has been presented that the ring-opening reaction takes place within ~2 ps followed by vibrational cooling of a hot ground state population which takes place on the 10 ps time scale. From the viewpoint of theory the large number of atoms in a fulgimide renders excited-state calculations difficult. However, a modification of the CHD/HT model for the application on fulgimides has been proposed in the literature.^{7,25}

Considering the much larger size and lower symmetry of a fulgimide, it is interesting to find out if the photophysics of a fulgimide can really be reduced to rather simple models like the ones depicted in Figure 1 involving a common excited state

(21) Handschuh, M.; Seibold, M.; Port, H.; Wolf, H. C. *J. Phys. Chem. A* **1997**, *101*, 502–506.
 (22) Port, H.; Gartner, P.; Hennrich, M.; Ramsteiner, I.; Schock, T. *Mol. Cryst. Liq. Cryst.* **2005**, *430*, 15–21.

(23) Malkmus, S.; Koller, F. O.; Heinz, B.; Schreier, W. J.; Schrader, T. E.; Zinth, W.; Schulz, C.; Dietrich, S.; Rück-Braun, K.; Braun, M. *Chem. Phys. Lett.* **2006**, *417*, 266–271.

(24) Koller, F. O.; Schreier, W. J.; Schrader, T. E.; Sieg, A.; Malkmus, S.; Schulz, C.; Dietrich, S.; Rück-Braun, K.; Zinth, W.; Braun, M. *J. Phys. Chem. A* **2006**, *110*, 12769–12776.

(25) Voll, J.; Kersch, T.; Geppert, D.; de Vivie-Riedle, R. *J. Photochem. Photobiol. A*, in press.

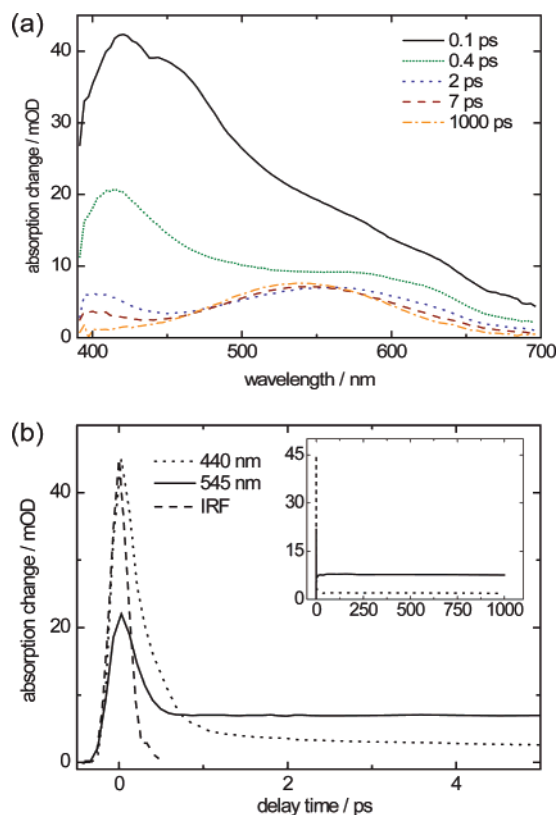


Figure 5. Transient absorption of the E-isomer after 387 nm excitation: (a) transient spectra taken at delay times as indicated; (b) absorption changes recorded at 440 and 545 nm up to 5 ps and 1 ns delay time (inset). The dashed line depicts the instrumental response function.

minimum. For a comprehensive understanding of such a photoreaction it is necessary to study both the ring-closure and the ring-opening reaction. Earlier experiments by S. T. Repinec et al. already revealed kinetic differences between a related photoinduced cyclization/cycloreversion.²⁶ With the present set of experiments we will show for the fulgimide system that cyclization/cycloreversion not only differ in terms of kinetics but also strongly in their time-dependent spectra. We use ultrafast transient absorption and fluorescence spectroscopy to track forward and backward pathways of the respective reactions. Whereas a transient absorption experiment is in principle sensitive to signatures of the educt and the product both in the ground and the excited state, fluorescence spectroscopy exclusively monitors the excited-state dynamics. We will show that the combination of both techniques is a powerful tool to reveal the topology of the relevant excited states.

2. Experimental

Synthesis of the *N*-methyl-indolyl-fulgimide will be published elsewhere. It has been characterized by NMR-spectroscopy and HPLC. In all experiments the fulgimide was dissolved in acetonitrile (Merck Uvasol). Flow-cuvettes were used to exchange the sample between consecutive laser shots. The solutions in the flow system were subject to steady-state illumination at appropriate wavelengths to regenerate the starting material which is lost by the photochemistry induced by the femtosecond excitation.

For the transient absorption experiments of the $C \rightarrow E$ reaction the sample was excited using pump-pulses at 540 nm with an energy of

150 nJ/pulse delivered by a home-built amplified laser system using a Ti:sapphire oscillator and a noncollinear optical parametric amplifier (NOPA).^{27,28} NOPA-generated probe light with magic angle polarization with respect to the pump beam was detected in multichannel fashion. The time-resolution of the setup was determined via cross-correlation between pump and probe beam using sum frequency generation and was 40 fs (fwhm) (for details see ref 29). The sample concentration was adjusted to an absorbance of ~ 1 OD at the pump wavelength for a 200 μm flow cell. The pulses were focused down to a beam waist of ~ 80 μm .

Transient absorption of the reaction $E \rightarrow C$ was recorded using the frequency doubled output of a Clark CPA2001 at 387 nm with an energy of 300 nJ/pulse for excitation focused down to a beam diameter of ~ 150 μm at the sample location. White light pulses with magic angle polarization with respect to the pump pulse were used as probe light and detected with a 1 kHz and 512 channel diode array.^{30,31} A time resolution of 200 fs (fwhm) was determined using the Kerr effect induced by the pump pulse in a solvent cuvette to gate the probe light. The absorption at the excitation wavelength was adjusted to ~ 1 OD for a 1 mm flow cell.

The (time-resolved) fluorescence was recorded using a Kerr shutter described in detail in ref 32. Briefly, a NOPA was used for excitation at 540 nm ($C \rightarrow E$), and the frequency doubled CPA output for excitation at 387 nm ($E \rightarrow C$). The excitation pulses had an energy of ~ 250 nJ/pulse and were focused down to a beam waist of ~ 150 μm . An optical parametric amplifier delivered gate pulses at 1100 nm with 28 μJ per pulse. Fluorescence light was detected using a CCD array, and the time-resolution of the setup was determined via cross-correlating strayed excitation light with the gate pulse. Values of 90 fs for the $C \rightarrow E$ and 140 fs for the $E \rightarrow C$ reaction were obtained. The flow cuvettes used had an optical path of 1 mm, and the optical density at the respective excitation wavelength was ~ 1.5 .

To derive quantitative information from the experiments the data were subject to a global fitting procedure. Here, we assume that the measured signal $S(\lambda, \tau)$ can be modeled using a sum of exponential decays convoluted with a Gaussian instrumental response function IRF:

$$S(\lambda, \tau) = \text{IRF} \otimes \left(\sum_{i=1}^n A_i(\lambda) e^{-(t-t_0(\lambda))/\tau_i} \right) \text{ with } t - t_0 \geq 0$$

Here, $A_i(\lambda)$ is the amplitude associated with the time constant τ_i at the wavelength λ . The IRF and the fwhm value of the respective experiments have been determined as stated above. Experimental dependencies of time zero $t_0(\lambda)$ due to group velocity dispersion in the setup have been thoroughly corrected for. The remaining variation of $t_0(\lambda)$ is supposed to account for spectral dynamics of the molecules such as a dynamic Stokes-shift which cannot be described by exponential kinetics. For time constants shorter than the IRF it is difficult to distinguish between an initial spectral shift and exponential dynamics. Here, we estimate the error of the time constants derived from the fitting procedure to be $\pm 30\%$. Otherwise a value of $\pm 30\%$ presents an upper limit for the uncertainty of the time constants.

3. Results

$E \rightarrow C$ Ring Closure. The steady-state fluorescence spectrum of the E-isomer is broad and structureless (Figure 3). Its maximum is red-shifted by ~ 9000 cm^{-1} with respect to the

- (27) Wilhelm, T.; Piel, J.; Riedle, E. *Opt. Lett.* **1997**, *22*, 1494–1496.
 (28) Riedle, E.; Beutter, M.; Piel, J.; Schenk, S.; Spörlein, S.; Zinth, W. *Appl. Phys. B* **2000**, *71*, 457–465.
 (29) Baigar, E.; Gilch, P.; Zinth, W.; Stöckl, M.; Härter, P.; von Feilitzsch, T.; Michel-Beyerle, M. E. *Chem. Phys. Lett.* **2002**, *352*, 176–184.
 (30) Huber, R.; Satzger, H.; Zinth, W.; Wachtveitl, J. *Opt. Commun.* **2001**, *194*, 443–448.
 (31) Laimgruber, S.; Schachenmayr, H.; Schmidt, B.; Zinth, W.; Gilch, P. *Appl. Phys. B* **2006**, *85*, 557–564.
 (32) Schmidt, B.; Laimgruber, S.; Zinth, W.; Gilch, P. *Appl. Phys. B* **2003**, *76*, 809–814.

(26) Repinec, S. T.; Sension, R. J.; Szarka, A. Z.; Hochstrasser, R. M. *J. Phys. Chem.* **1991**, *95*, 10380–10385.

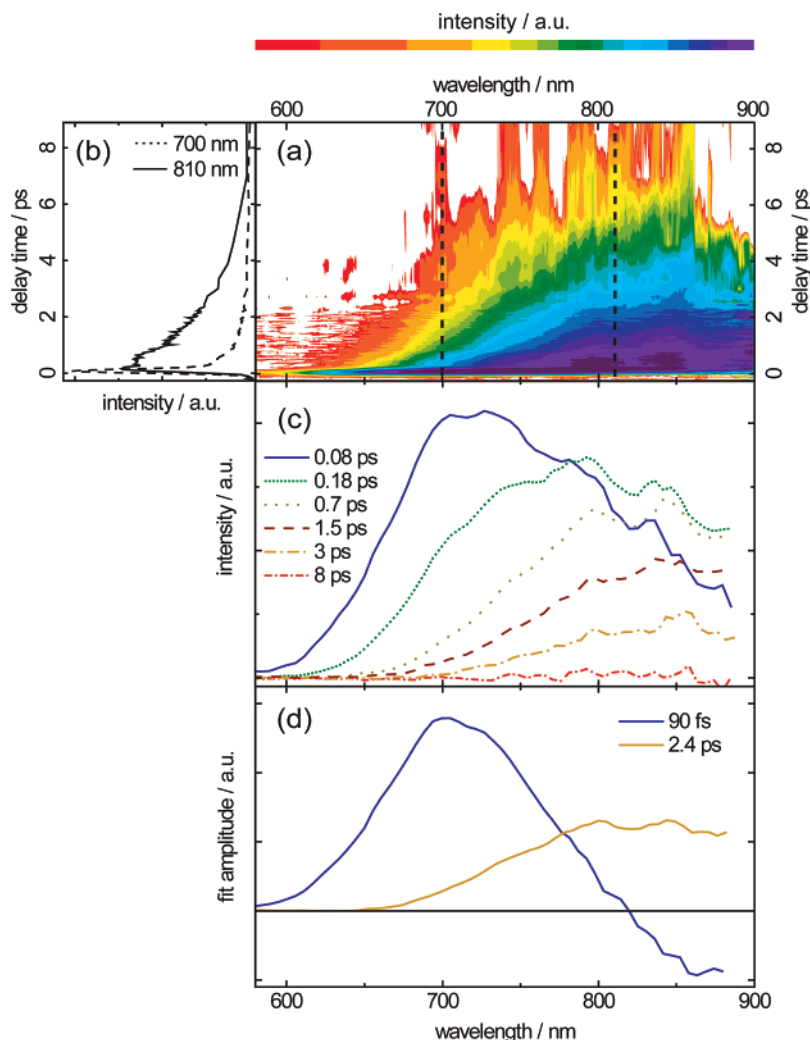


Figure 6. Femtosecond fluorescence experiment on the C-isomer after 540 nm excitation. (a) Contour plot of the transient fluorescence. The dashed lines indicate the wavelengths which are plotted in panel b. (b) Decay of the signal at 810 nm (solid line) and 700 nm (dashed line). (c) Transient fluorescence spectra taken at delay times as indicated. (d) Decay-associated spectra of the time constants retrieved from a global analysis.

maximum of the first absorption band. The transient fluorescence of the E-isomer observed after photoexcitation at 387 nm shows the following features (Figure 4): It initially peaks around 450 nm. (The spike at 438 nm at early delay times is due to Raman scattering of the solvent.) In this spectral range the decay time of the fluorescence is shorter than the instrumental response time of 140 fs. After this initial rapid decay a weak fluorescence spectrum peaking at 520 nm is detected. Furthermore, the onset of the signal in the very red wing of the fluorescence occurs approximately 100 fs later than at the blue edge of the emission (see Figure 4b). The data is analyzed using the global fitting procedure described above. A nice agreement between fit and experiment is found using two decay functions with time constants of 55 and 350 fs. Over the fitted spectral range from 410 to 740 nm the onset of the fitting function is shifted toward later delay times by ~ 100 fs. The existence of a longer-lived fluorescence component can be excluded since the steady-state fluorescence spectrum can be reproduced by time integrating the transient signal. When comparing the amplitudes of the two decay components it has to be taken into account that the fast component has a time constant which is below the instrumental response function. As a consequence the contribution of the fast

(55 fs) component to the fluorescence emission (Figure 4c) is strongly suppressed as compared to the one of the 350 fs component. The fitting routine of course accounts for this effect and delivers “correct” decay-associated spectra (Figure 4d). These spectra indicate that the peak amplitude associated with the 55 fs dynamic exceeds the one of the 350 fs component by a factor of ~ 30 . If both processes were assigned to the decay of different electronic states their relative oscillator strengths can be estimated by comparing the integrated decay-associated spectra. This integration is subject to uncertainties since (i) the 55 fs component is shorter than the instrumental response function and (ii) the spectral correction necessary prior to integration significantly distorts the weak signal in the red wing of both spectra (Figure 4d). (The spectral integration requires a λ^2 factor for the wavelength to frequency transformation and another λ^3 factor to account for the wavelength dependence of the spontaneous emission.³³) Nevertheless, a very strong difference between the integrated spectra results: The oscillator strength of the short-lived emission is at least ten times larger than that of the longer-lived component.

In the corresponding transient absorption experiment a very broad induced absorption band peaking at 420 nm appears

immediately after excitation at 387 nm (Figure 5). This signal decays within a few hundred femtoseconds leaving an offset absorption around 400 and 600 nm. The signal at 400 nm disappears within some picoseconds whereas the 600 nm signal contribution blueshifts on the same time scale and afterward stays constant until the end of the covered time range (1 ns). A global analysis of the data is performed in the same manner as described above. It leads to a triple exponential decay of the induced absorption band with time constants of 150 fs, 400 fs, and 7 ps. Within the experimental error the 400 fs time constant matches the slow time constant found in the fluorescence experiment whereas the fast time constants found in both experiments clearly differ from each other. The offset spectrum at 1 ns delay time virtually matches the steady state difference spectrum of the C- and the E-isomers. Most of the features of this offset spectrum are already present after ~ 2 ps. The deviations between the 2 ps and the 1 ns spectra (Figure 5a) bear the characteristics of a vibrationally hot molecule (broadening and redshift of absorption). The spectra at early times transform into the 1 ns spectrum with a characteristic time of 7 ps typical for vibrational cooling. Consequently, the 400 fs process has to be associated with product formation and re-formation of the starting material.

C \rightarrow E Ring Opening. The steady-state fluorescence spectrum of the C-isomer is unstructured and extends from ~ 650 nm to the infrared beyond 1000 nm (Figure 3). Its maximum is red-shifted by ~ 6400 cm^{-1} with respect to the maximum of the visible electronic absorption band. The maxima of the fluorescence spectra of the E-isomer and the C-isomer are apart from each other by ~ 7500 cm^{-1} and also differ in shape. The fluorescence dynamics of the C-isomer are recorded after excitation at 540 nm (see Figure 6). At early delay times the fluorescence signal is centered around 700 nm. The consecutive dynamics are difficult to unravel as several processes occur at the same time: The decay of the fluorescence amplitude takes place on two different timescales and is superimposed with a spectral redshift of the signal. The decay of the fast component which is most pronounced around 700 nm proceeds within the instrumental response time of 90 fs. The second component is spectrally centered around 850 nm and decays within a few picoseconds (Figure 6b,c). The redshift of the signal takes place within ~ 0.5 ps and moves the fluorescence maximum by ~ 2500 cm^{-1} with respect to its initial spectral position. Additionally, a recurrence at a delay time of ~ 400 fs is superimposed to the exponential dynamics (only weakly visible in the data representation chosen here). After a delay time of ~ 10 ps the fluorescence decay is terminated. Again a contribution of a long-lived fluorescence component can be excluded as time integration of the transient signal reproduces the steady-state fluorescence spectrum. Both, the dynamic shift and the recurrence of the signal are non-exponential processes. As a consequence a global fitting procedure as the one we have performed on the fluorescence data of the E-isomer is rendered difficult. Nevertheless, to quantify the fluorescence decay time we have used the global fitting procedure starting at a delay time of 1.2 ps. From that time on the non-exponential signal contributions can be neglected and a nice agreement between the data and the fit is obtained using a single exponential decay function with a time constant of 2.4 ps. With that value set as a fixed parameter we repeated the global analysis using the complete dataset to

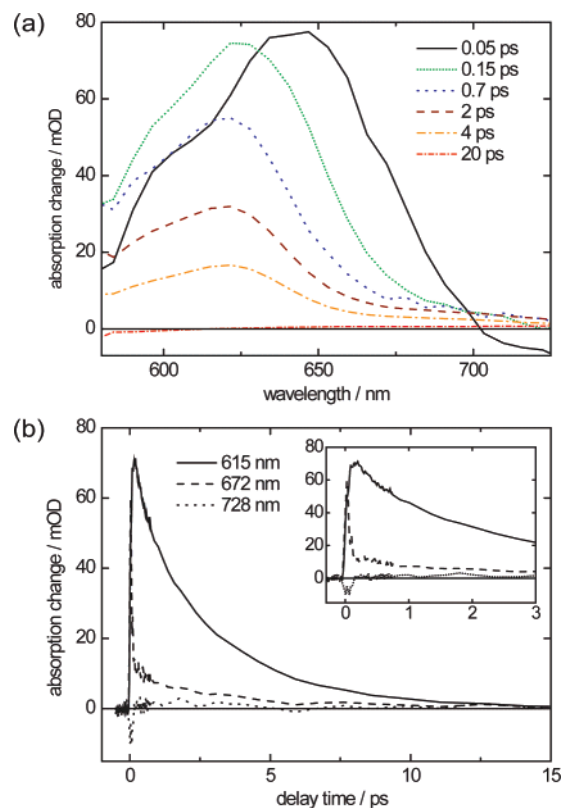


Figure 7. Transient absorption of the C-isomer after 540 nm excitation: (a) transient spectra recorded at delay times as indicated; (b) transient absorption changes at 615 nm (solid line), 672 nm (dashed), and 728 nm (dotted) plotted up to 15 and 3 ps delay time (inset).

also retrieve the decay-associated spectrum of the sub 100 fs process. Here, a nominal time constant of 90 fs is assigned to this process and the maxima of both decay-associated spectra obtained in that manner (Figure 6d) are by ~ 2000 cm^{-1} apart from each other. The delayed rise of the fluorescence signal in the red wing of the spectrum is reflected in the negative-fit amplitude in this spectral range.

The transient absorption of the C-isomer features a broad induced absorption centered around 650 nm which appears immediately after photoexcitation (Figure 7). Within ~ 200 fs this absorption band shifts toward shorter wavelengths. Afterward it decays on the time scale of several picoseconds. Initially, a small negative signal amplitude which decays within ~ 80 fs is observed at wavelengths greater than 700 nm. Similar to the observations in the fluorescence experiment a recurrence of the transient absorption signal can be seen at 300–400 fs delay time. We have analyzed the data in the same manner as the C-isomer fluorescence using a global fit starting at a later delay time (1 ps) and discarding the non-exponential signal contributions. Here, using a double exponential decay function with time constants of 2.4 and 8.0 ps nicely reproduces the experimental data. As the 2.4 ps time constant matches the lifetime of the slowest emission component it can be assigned to the decay of excited-state absorption. As reported earlier²³ this time constant matches the one of the product formation. Vibrationally excited starting material (C-isomer) which is formed after internal conversion should absorb in the probed spectral range. Consequently, we assign the 8 ps time constant to vibrational cooling of hot ground-state population of the C-isomer.

4. Discussion

We have compared a photoinduced ring closure ($E \rightarrow C$) with the corresponding cycloreversion ($C \rightarrow E$) by means of femtosecond fluorescence and absorption spectroscopy. The kinetics of the two photoreactions bear similarities but also very distinct differences. For either direction the fluorescence decay is biphasic. In the blue part of the respective spectrum a sub 100 fs decay is observed, whereas in the red part the decay is substantially slower. The time constants of the slower processes are also observed in the absorption experiment and there mark the formation of the respective photoproduct. The absorption experiments additionally show dynamics in the ~ 10 ps range which can be attributed to vibrational cooling processes of hot ground-state species. The product formation time is by a factor of 6 larger for the $C \rightarrow E$ ring opening than for the $E \rightarrow C$ ring closure. The fluorescence spectra associated with the excited-state depletion also show pronounced differences: In the $E \rightarrow C$ case the spectrum peaks at ~ 525 nm, whereas the maximum of the $C \rightarrow E$ spectrum is located at ~ 840 nm. So the peaks are ~ 7000 cm^{-1} apart. Furthermore, in the $E \rightarrow C$ case the amplitude of the slower fluorescence component (~ 400 fs) is by a factor of ~ 0.03 weaker than that of the fast component (< 100 fs). In the $C \rightarrow E$ direction the amplitudes of both components are similar.

Implications of these findings will be now discussed using the reaction models presented in the Introduction as a guideline. The simplest model uses only one reactive coordinate and involves one excited state (i) (Figure 1a). This corresponds to the often used Woodward–Hoffmann scheme with an avoided crossing between ground and excited state. A one-dimensional model with two excited states (ii) (Figure 1b) can be regarded as an extension of model i and has been suggested for the photophysics of the CHD/HT system. A further extension can be made to a multidimensional model (iii) involving one or more excited states.

In model i photoexcitation of the E- and C-isomer should at first result in fluorescence emission from the respective Franck–Condon points. Since the low energy absorption bands of the two isomers peak at different frequencies (Figure 3), different wavelengths for the Franck–Condon emission are also expected and observed. But subsequently, the isomers would deform to arrive at the *common* minimum on the excited-state surface. In the course of this motion the fluorescence properties of the two isomers should converge. The fluorescence spectra at this latter stage should be identical (or at least similar) in terms of emission frequency and intensity. Additionally, the slower components of the fluorescence decay representing the excited-state depletion should be identical. All these predictions do not match our observations. As a consequence model i has to be ruled out.

In model ii photoexcitation promotes both isomers to the optically bright $1B_2$ state (Figure 1b). Along the reaction coordinate the $2A_1$ state crosses the $1B_2$ state twice. The $2A_1$ state is the electronic state which in the Woodward–Hoffmann sense correlates with the ground state. The sub 100 fs process for either direction might be associated with the transition from a $1B_2$ -like state to a $2A_1$ -like state. (Please note that due to the low symmetry the electronic states of the fulgimides can actually not be named as A, B etc. For the sake of clarity we will keep this nomenclature while comparing the fulgimide and the CHD/HT system.) Different time constants for the $C \rightarrow E$ (90 fs) as

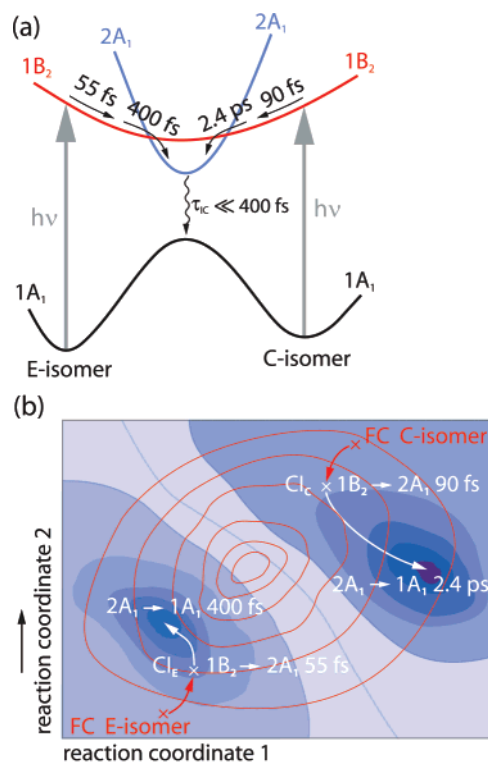


Figure 8. Schematics of a (a) one-dimensional and (b) two-dimensional model for the investigated cyclization/cycloreversion: (a) After excitation to the $1B_2$ state (red line) the isomers experience non-Condon effects (55 fs/90 fs) modulating the fluorescence intensity followed by internal conversion to the $2A_1$ state (400 fs/2.4 ps, blue line). (b) Starting from the respective Franck–Condon geometries (FC) on the $1B_2$ state (red lines) the isomers undergo internal conversion to the excited $2A_1$ state (55 fs/90 fs, blue lines) at two different conical intersections CI_E and CI_C . On the $2A_1$ surface both isomers access different minima (deep blue) from which they undergo further internal conversion to the $1A_1$ ground state (400 fs/2.4 ps). These minima mark the branching points for the respective photoreaction.

compared to the $E \rightarrow C$ direction (55 fs) could be due to different crossing points. Yet, after the internal conversion to the $2A_1$ state the two isomers should deform toward a *common* minimum. As argued above this scenario would lead to similar fluorescence properties for both isomers which are not observed. Only a re-assignment of the time constants could “save” a one-dimensional model. Here, the sub 100 fs processes would be associated with the motion of the molecules out of the Franck–Condon region (Figure 8a) resulting in the observed red shift of the fluorescence emission. The concomitant decrease in fluorescence intensity would then indicate a dependence of the oscillator strength on the nuclear coordinates. Such non-Condon effects have been proposed to be operative in many molecules undergoing ultrafast internal conversion or photochemistry.^{34–36} There, it has also been found that the emission decay can be faster than the reduction of excited-state absorption.³⁴ That could explain the difference which we observe between the shortest time constant in the absorption (~ 150 fs) and the fluorescence experiment (55 fs) for the $E \rightarrow C$ reaction. The slower

(33) Birks, J. B., Ed. *Photophysics of Aromatic Molecules*; Wiley-Interscience: London, New York, Sydney, Toronto, 1970.

(34) Kovalenko, S.; Schanz, R.; Farztdinov, V.; Hennig, H.; Ernsting, N. *Chem. Phys. Lett.* **2000**, *323*, 312–322.

(35) Schmidt, B.; Sobotta, C.; Malkmus, S.; Laimgruber, S.; Braun, M.; Zinth, W.; Gilch, P. *J. Phys. Chem. A* **2004**, *108*, 4399–4404.

(36) Rubtsov, I. V.; Yoshihara, K. *J. Chin. Chem. Soc.* **2000**, *47*, 673–677.

components of the fluorescence decay would then be associated with the transfer to the $2A_1$ state (Figure 8a). The ensuing depletion of this state to the ground state might be faster than its population and would then not be observed. So the experimental observation can be “forced” to fit a one-dimensional model. Yet, some consequences of that “forcing” render the model unlikely. The initial ultrafast process reduces the fluorescence intensity by a factor of 0.03 for the $E \rightarrow C$ direction and only slightly changes that intensity for the other direction. So the $E \rightarrow C$ reaction would involve a strong non-Condon effect and the $C \rightarrow E$ reaction nearly none. Presently, we are not aware of a rationale for such a huge difference. In addition, within this model the non-adiabatic couplings mediating the transfer from the $1B_2$ state to the $2A_1$ state must be substantially different to account for the different transfer time constants. Obviously, also the involvement of even more electronically excited states might account for our observations. Yet, as outlined in the following a multidimensional view leads to a simpler explanation.

As to model iii, while we cannot finally rule out one-dimensional models we conclude from the above considerations that a multidimensional model is more appropriate. In two dimensions a possible model could be as follows: A reactive space is spanned by two reaction coordinates and again involves two electronically excited states (Figure 8b). This enables the two isomers to move along different reaction paths. After photoexcitation the isomers start to evolve on the $1B_2$ potential energy surface (red lines in Figure 8b) at their respective Franck–Condon geometries to arrive at two different conical intersections (CI_E , CI_C) with the $2A_1$ state (depicted in blue in Figure 8b). The $1B_2 \rightarrow 2A_1$ internal conversions at these conical intersections would then be associated with the sub 100 fs processes observed for both reactions. If the $2A_1$ state features *two minima* which are selectively accessed during the two reactions an explanation for our observations is close at hand: After the $1B_2 \rightarrow 2A_1$ internal conversion the isomers arrive at their respective minimum on the $2A_1$ state from which internal conversion to the ground state takes place. These minima mark the branching points for product formation or back reaction to the starting material. The existence of two different branching points instead of only one would account for the large spectral and temporal deviations in the fluorescence and product formation times (400 fs/2.4 ps) in the cyclization/cycloreversion.

A similar two-dimensional model has been suggested for the CHD/HT system by Geppert et al. using quantum dynamics simulations.⁷ Here, a reactive space is proposed using two well-chosen reaction coordinates, namely, a distance and a dihedral vector. Within this reactive space two conical intersections with the ground state exist which mark the respective branching points for the photoreactions. One of these conical intersections

lies close to the excited-state minimum. Remarkably, the calculations show that the cyclization accesses only this very conical intersection almost exclusively whereas cycloreversion proceeds preferentially via the other conical intersection. This matches our experimental findings. For the extension of this model to a fulgimide it is assumed that because of the larger size of such a system several strongly mixed electronic states of lower symmetry than in the CHD/HT system are involved.⁷ Thus, it is likely that the $2A_1$ state which is optically dark in the CHD/HT system carries some oscillator strength in the fulgimide and is consequently responsible for slow fluorescence components we observe (400 fs/2.4 ps). More recent theoretical results indicate the existence of an additional minimum in the excited-state of a fulgimide which lies close to the Franck–Condon geometry of the C-isomer.²⁵ In these calculations the $1B_2$ and the $2A_1$ states are combined into one adiabatic surface and therefore the $1B_2 \rightarrow 2A_1$ internal conversion is not treated explicitly. Nevertheless, the theoretical results substantiate the idea that, contrary to the simplified and the extended Woodward–Hoffmann scheme (Figure 1), the $E \rightarrow C$ and $C \rightarrow E$ reactions use different pathways on the excited-state potential-energy surfaces and no common excited-state minimum is accessed. That can account for the spectral and dynamical deviations in the fluorescence behavior of both isomers which prevail throughout the photoreaction as well as the different product formation times (400 fs/2.4 ps).

5. Conclusion

We have investigated electrocyclic ring-opening and -closure reactions in a photochromic fulgimide by means of ultrafast absorption and fluorescence spectroscopy. A biphasic fluorescence decay is common for both isomers and points to a sequential mechanism involving two excited electronic states. The fluorescence decay times and spectra as well as the product formation times significantly differ from each other for both isomers. That rules out a simple one-dimensional reaction scheme unless strong non-Condon effects are involved. As an explanation for our observations we suggest an adaption of theoretical results on fulgimides and their chromophore, the CHD/HT system. Here, a two-dimensional reactive space involves the participation of conical intersections which lie along the reactive pathway in the excited state and are selectively accessed by the photoexcited isomers.

Acknowledgment. The authors are thankful to Prof. R. de Vivie-Riedle and D. Geppert for stimulating discussions. B. Heinz appreciates a scholarship of the Fonds der Chemischen Industrie.

JA071396I